climate

MDPI

Article

Heat Vulnerability Index Mapping: A Case Study of a Medium-Sized City (Amiens)

Aiman Mazhar Qureshi and Ahmed Rachid *

Laboratory of Innovative Technologies, University of Picardie Jules Verne, 80000 Amiens, France; aimanmazhar.qureshi@gmail.com

* Correspondence: ahmed.rachid@u-picardie.fr

Abstract: Urbanization, anthropogenic activities, and social determinants such as poverty and literacy rate greatly contribute to heat-related mortalities. The 2003 strong heat wave (Lucifer) in France resulted in catastrophic health consequences in the region that may be attributed to urbanization and other anthropogenic activities. Amiens is a medium-sized French city, where the average temperature has increased since the year 2000. In this study, we evaluated the Heat Vulnerability Index (HVI) in Amiens for extreme heat days recorded during three years (2018–2020). We used the principal component analysis (PCA) technique for fine-scale vulnerability mapping. The main types of considered data included (a) socioeconomic and demographic data, (b) air pollution, (c) land use and cover, (d) elderly heat illness, (e) social vulnerability, and (f) remote sensing data (land surface temperature (LST), mean elevation, normalized difference vegetation index (NDVI), and normalized difference water index (NDWI)). The output maps identified the hot zones through comprehensive GIS analysis. The resultant maps showed that high HVI exists in three typical areas: (1) areas with dense population and low vegetation, (2) areas with artificial surfaces (built-up areas), and (3) industrial zones. Low-HVI areas are in natural landscapes such as rivers and grasslands. Our analysis can be implemented in other cities to highlight areas at high risk of extreme heat and air pollution.

Keywords: Heat Vulnerability Index; heat mapping; heat illness; remote sensing; GIS

Citation: Qureshi, A.M.; Rachid, A. Heat Vulnerability Index Mapping: A Case Study of a Medium-Sized City (Amiens). *Climate* **2022**, *10*, 113. https://doi.org/10.3390/cli10080113

Academic Editor: Mário Gonzalez Pereira

Received: 17 June 2022
Accepted: 20 July 2022
Published: 24 July 2022

1. Introduction

Climate change has greatly impacted the global mean temperatures and has resulted in strong heat waves during the last couple of decades. It has been responsible for heat-related morbidities and mortalities globally, including heat waves in the Balkans (2007), the Midwestern United States (1980), France (2003), and Russia (2010) [1,2]. In August 2003, France was hit by a strong heat wave named Lucifer, with catastrophic health consequences. Heat events, as well as socioeconomic vulnerability, led to more than 14,800 mortalities in France due to dehydration, hyperthermia, and heat stroke [3]. Heat waves with urban heat islands can increase the death ratio, particularly for vulnerable people such as outdoor workers and elders who are socially isolated and/or with pre-existing disease [4,5]. Other influencing factors include urbanization, poverty, literacy rate, and possibly air pollution [6,7]. According to the World Health Organization (WHO), a 2 °C increase in the apparent temperature (AT) is a limiting warning that can prevent rising heat mortalities, but later studies proved that heat events are inevitable even if the global heat stress warning is restricted to 2 °C AT [8]. Mortality risk in France can be increased by 1–1.9 log for every 1 °C AT. Long heat waves (more than 5 days) have an impact of 1.5–5 times greater than shorter events [9]. Urbanization promotes anthropogenic activities which lead to heat events. Adaptive strategies are necessary to protect the residents from heat-related events and health risks in the coming years.

Amiens is a medium-sized city in northern France, crossed by the Somme River. The hot season lasts 3 months, from June to August, where maximum air temperatures can

reach 41 °C [10]. The hottest month of the year in Amiens is July. It has been reported that the mean annual air temperature between 2000 and 2018 increased by 1 °C above the 20th century average, with 2003, 2011, 2014, 2017, and 2018 being the warmest years [11]. This threat of extreme heat events is likely to increase due to the combined effects of global warming and rapid urbanization in the future. Although the data related to the strong 2003 heat wave and associated adverse health outcomes have been evaluated previously [12], the Heat Vulnerability Index (HVI) was recently investigated for big cities, e.g., Camden, Philadelphia [13], London [14], and Sydney [15], where the influence of air quality was not considered except for the study presented by Sabrin for Camden [16]. To our best knowledge, there are no studies addressing the impact of heat waves on a medium-sized city using the HVI approach, where the population is less than one million. Within this context, the current study aimed to identify the heat-vulnerable communities and areas in Amiens where heat stress mitigation strategies are required. The main data types which we used for this study to develop the HVI model were (a) socioeconomic and demographic data, (b) air pollution, (c) land use and land cover, (d) elderly heat illness, (e) social vulnerability, and (f) satellite data (land surface temperature and mean elevation).

Heat maps of high spatial and temporal resolution are generated from satellite data, and HVI maps are derived using principal component analysis (PCA) to help urban planners and public health professionals to identify places at high risk of extreme heat and air pollution. This case study aims to bring attention to the fact that medium-size cities are also vulnerable to heat, requiring some proactive measures against future extreme heat events. Our suggested index can be a useful tool in decision making for dealing with extreme events and can guide city planners and municipalities.

The paper is organized as follows: the methodology is presented in Section 2 with data analysis and the developed working model. It also provides the information of the used technique and the influence of components. The obtained results and HVI map with valuable information are given in Sections 3 and 4, respectively. The paper ends with a conclusion in Section 5, with some perspectives and recommendations in Section 6.

2. Materials and Methods

Several parameters have been studied that have a possible correlation with extreme heat events and air pollution in urban settings, which were identified and discussed in the previous literature to develop our conceptual model [14,17]. The methodology for the case study was developed as a working model for HVI mapping, as shown in Figure 1. In this study, risk factors such as social vulnerability (factors taken from the literature) and the environment (identified after extreme event analysis of the studied area) are discussed in this section.

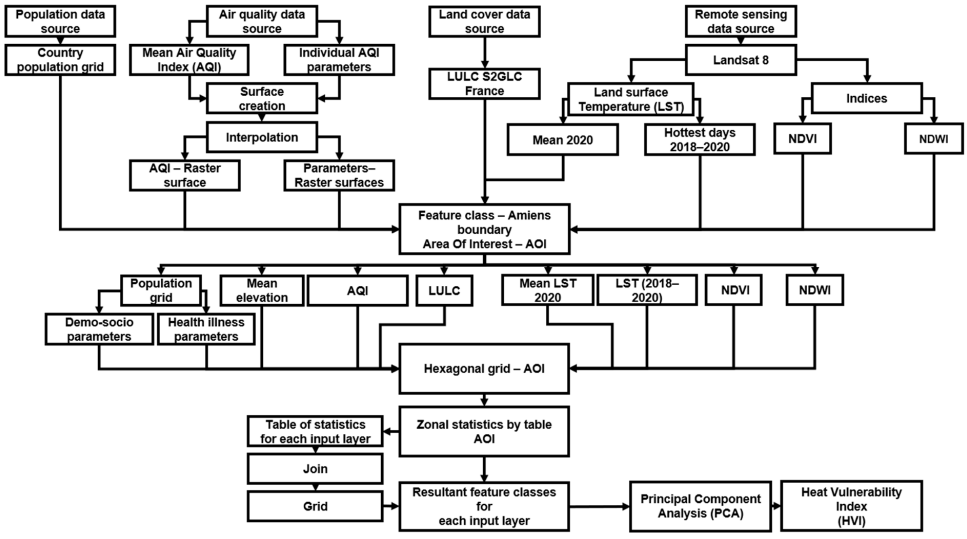

Figure 1. Working model for Heat Vulnerability Index mapping of Amiens.

2.1. Identification of Risk Factors

2.1.1. Social Vulnerability Factors (SVF)

Age, pre-existing medical conditions, and social deprivation are among the various key factors that make people likely to experience more adverse health outcomes related to extreme temperatures. References were used for the population density, poverty rate, illiteracy rate, vulnerable age group, illness rate (asthma, cardiovascular disease, and respiratory disease other than asthma), and isolated elderly (living alone in the summer), as presented in Table 1.

Mapping for the socially vulnerable population was performed using a dataset from world pop [18], which provides a population at a map scale of 100 m. Hexagon grids of 5 ha were generated in the area of Amiens city. Zonal statistics was used to extract the population at the grid level to maintain homogeneity of analysis throughout the study. In addition, a multi-frame population map of a specific group was also created, as presented in Figure 2.

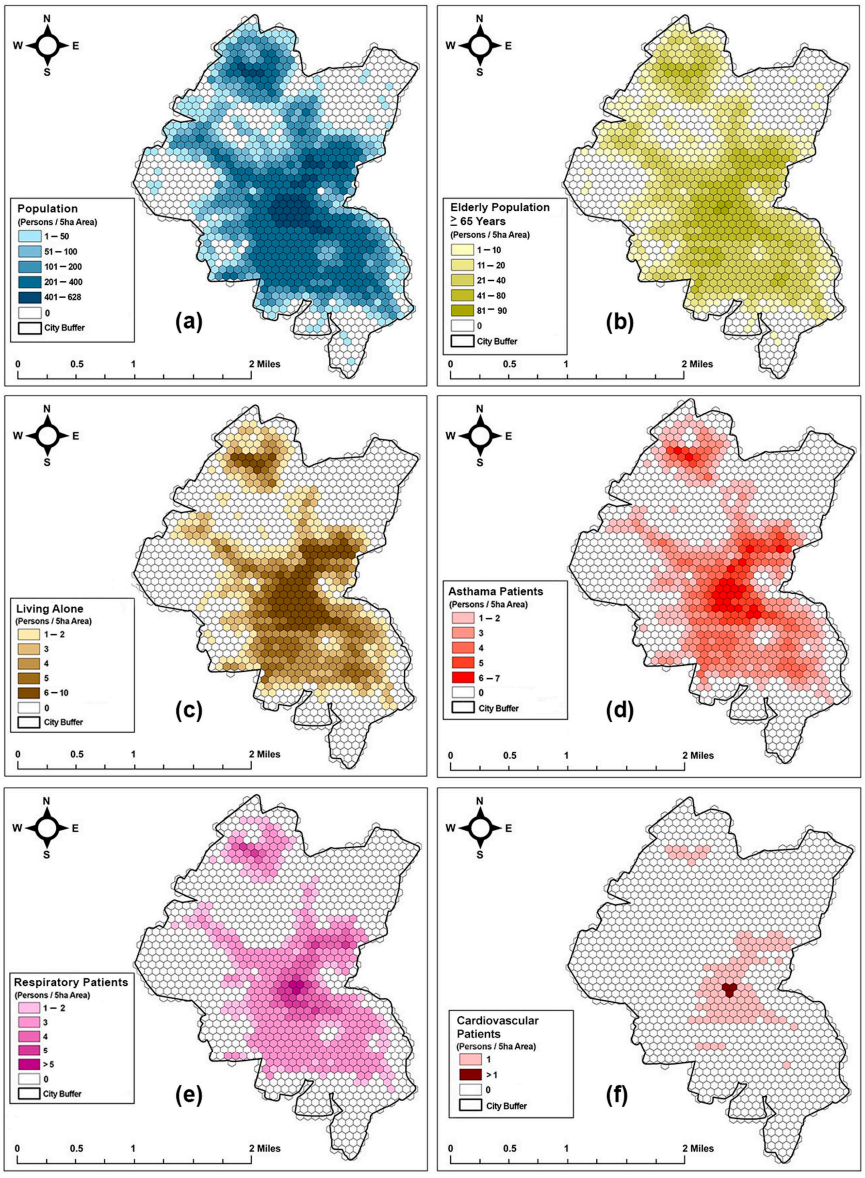

Figure 2. (**a**) Total population in the city; (**b**) elderly population ≥65 years; (**c**) those living alone; (**d**) asthma patients; (**e**) patients with other respiratory diseases; (**f**) cardiovascular patients.

Table 1. Estimation of social vulnerability factors

Factors	Estimated Statistics	Year	Source	Reference
Poverty rate	15% (17,045 habitants)	2020	French Newspaper "Courrier Picard" 2020	-
Elderly population >65	19% (25,246)	2014	National Institute of Statistics in France—INSEE	[19]
Illiteracy rate (no diploma aged >15 years)	22%	2015	Municipality of Amiens City population	[20]
Illness ratio of the elderly population	28 out of every 200 patients	2000	Insurance company survey	[21]
Cardiovascular patients	799 Elder = 112	2008	Research paper	[22]
Asthma patients	8% Total = (10,629) Elders = 1400	2014	Eurostat	[23,24]
Other respiratory diseases excluding asthma	6% Total = 7972 Elders = 1100			
Socially vulnerable elders in the summer	2000	2014	Article: "The city of Amiens watches over our seniors"	[25]

Note: The statistical data from referenced sources give the rough estimation of social vulnerability.

2.1.2. Extreme Event Analysis

To identify the extreme events recorded, the hourly data for the summer (July and August) were collected from Météo France [10] and Atmo France [26]. Data were analyzed by dividing them into categories to estimate risk alerts. The Météo France weather station is located in Amiens Glisy, 14 km from the city center. Three air pollution stations are located in different areas (details for data recording are given in Table A1). The geographical locations of air pollution and weather stations can be seen in Figure 3. Weather data were analyzed to assess the levels and duration of heat episodes. The assumption scale was made by categorizing air temperature ranges into risk warnings: slightly warm (26–30 °C), warm (31–36 °C), and very hot (37–41 °C). This approach made it possible to analyze the huge hourly data during the summer seasons of 2018–2020. The number of hours of heat stress with their levels is presented in Figure 4.

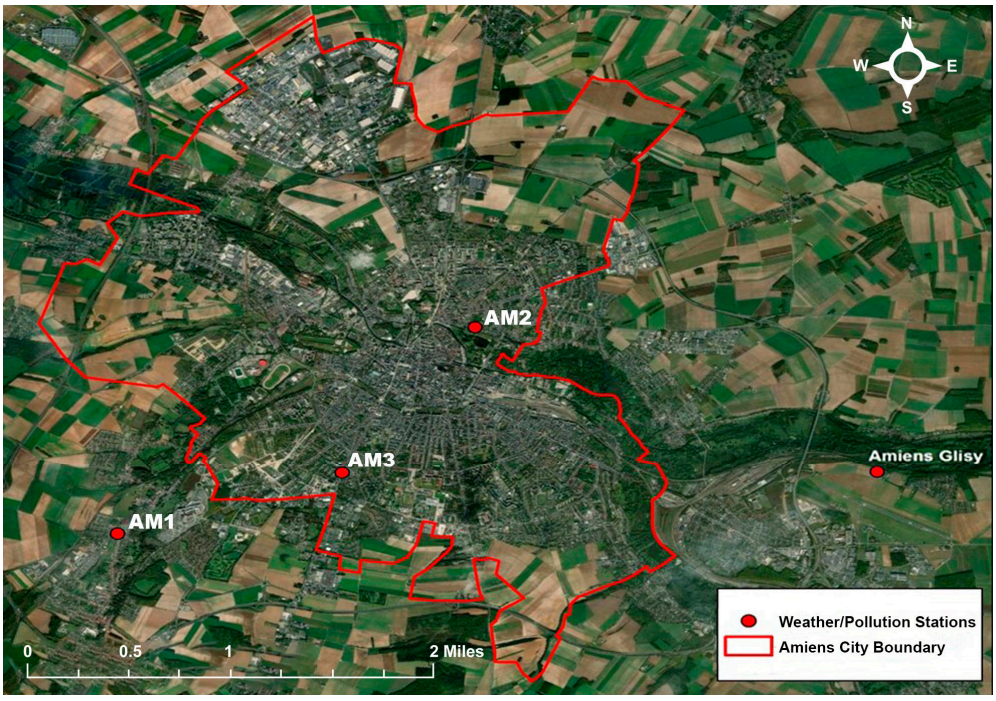

Figure 3. The geographical locations of air pollution and weather stations.

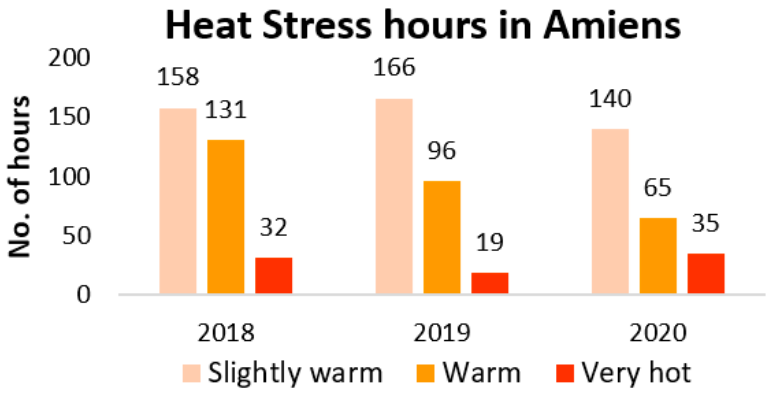

Figure 4. Heat stress hours in Amiens (data source: Meteo France).

The air quality data were obtained over the past 10 years from local monitoring stations referred to as AM1, AM2, and AM3, where certain non-regularization of monitoring was noticed, particularly in the AM3 station (details are provided in Table A1). The temperature (ambient and surface) and air quality data were analyzed for a correlation study from 2018 to 2020, and it was observed that, due to the irregularity, the air quality data of 2018 were not sufficient. However, data from 2019 and 2020 were adequate for this study. The correlation coefficients are plotted in Figure 5, showing that anthropogenic activities also increased the frequency and intensity of extreme heat. Moreover, a significant relationship was observed between heat events and ground-level ozone, representing the motivation of this research.

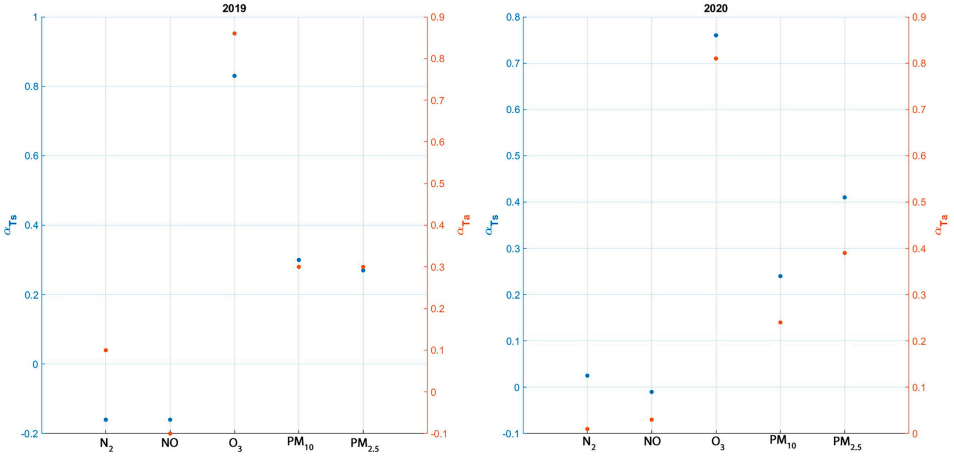

Figure 5. Correlation coefficient (α) of monitored air temperature (Ta) and surface temperature (Ts) with air pollutants during summer season (July and August) of 2019 and 2020 (data source ATMO France).

2.1.3. Environmental Risk Factors

After analyzing the collected data, it was found that low air quality and an increase in temperature are risk factors that depend on urban geometry, the proportion of urban greenery, and materials. In current study, the main environmental risk factors of these three were are considered and mapped for the identification of heat-vulnerable areas. Further details are provided in the subsections below.

a. LST mapping of extreme heat days

Data for environmental risk factors such as land surface temperature (LST), normalized difference vegetation index (NDVI), and normalized difference water index (NDWI) were first collected in the area of study to create vulnerability maps. The city suffers from a lack of canopy-scale temperature readings, air quality data, and consistent weather stations,

which limited us to studying the spatial patterns of temperature and pollution in the city at high resolution. We only had data from one meteorological station, which was insufficient to achieve realistic and reliable data for spatial distribution. The city mainly relies on weather stations located outside the city for weather forecasts. Thus, temperature data were collected at fine spatial scales via the Landsat 8 earth observation satellite [27], which integrates the role of the built environment. Satellite data can be used to derive the surface temperature using high-spatial-resolution imagery and remote sensing techniques to study the effect of heat over a large area. Therefore, we used Landsat 8 multispectral satellite images to obtain high-resolution LST, NDVI, and NDWI data using Equations (1–4). The mean LST values at the pixel level show that Amiens experienced high LST on 27 July 2018, 25 July 2019, and 31 July 2020. Landsat 8 images were used to derive the LST raster layers. The maps appear to show regions with higher temperatures between 20 °C and 41.5 °C. The summer 2020 (July and August) mean LST map was also derived because last year is considered highly relatable for expected coming heat events. The derived maps are presented in Figure 6.

$$\mathrm{LST} = \frac{\mathrm{T_{sensor}}}{1 + (\lambda \times (\mathrm{T_{sensor}} / \beta)) \ln(\varepsilon)} \quad (1)$$

where LST is the land surface temperature, and $\mathrm{T_{sensor}}$ is the band 10 brightness temperature in K, later converted into °C [28], λ is the wavelength of the emitted radiance in meters, $\beta = 1.438 \times 10^{-2}$ Mk, and ε is the surface emissivity [29].

$$\mathrm{NDVI} = \frac{(\mathrm{NIR} - \mathrm{RED})}{(\mathrm{NIR} + \mathrm{RED})} \quad (2)$$

$$\mathrm{NDWI} = \frac{\mathrm{G} - \mathrm{NIR}}{\mathrm{G} + \mathrm{NIR}} \quad (3)$$

where NIR is the near-infrared waveband (band 5 for Landsat 8), RED channels of remotely sensed images are the reflectance of the visible red waveband (band 4 for Landsat 8), and G represents the green channels.

For ε, it is necessary to correct the spectral emissivity using the NDVI value.

$$\varepsilon = 1 + 0.047 \ln(\mathrm{NDVI}),\ 0 \leq \mathrm{NDVI} < 0.15 \quad (4)$$

In previous studies [30], mean elevation was taken as an indicator of PCA. In this study, altitude was considered an important factor in temperature distribution. The elevation was taken from the Shuttle Radar Topography Mission (SRTM) 30 m pixel raster data. This elevation of the terrain was used to visualize and analyze the flat or mountainous distribution areas.

b. Land use and land cover (LULC)

It can be observed that a large scattered hot area existed in the center of the city. The high LST was mainly distributed in the built-up areas of Amiens. These areas were combined with a land use/land cover map (Figure 7), and it was recognized that the high LST was mostly distributed in the following areas: (i) densely populated areas, (ii) areas with low vegetation coverage, (iii) areas with artificial surfaces, and (iv) industrial zones.

However, low-LST areas were mainly located in natural landscapes, such as rivers and grasslands. The LULC ratio of Amiens is shown in Table 2.

c. Air quality

The Air Quality Index (AQI) for 2019 and 2020 for the summer season (July–August) was estimated using the AQI calculator [31]. The inverse distance weighted (IDW) interpolation method was used to create the AQI surface to develop the maps in Figure 8. Additional layers of each raw pollution variable were also created, which were later used in the PCA for HVI calculations.

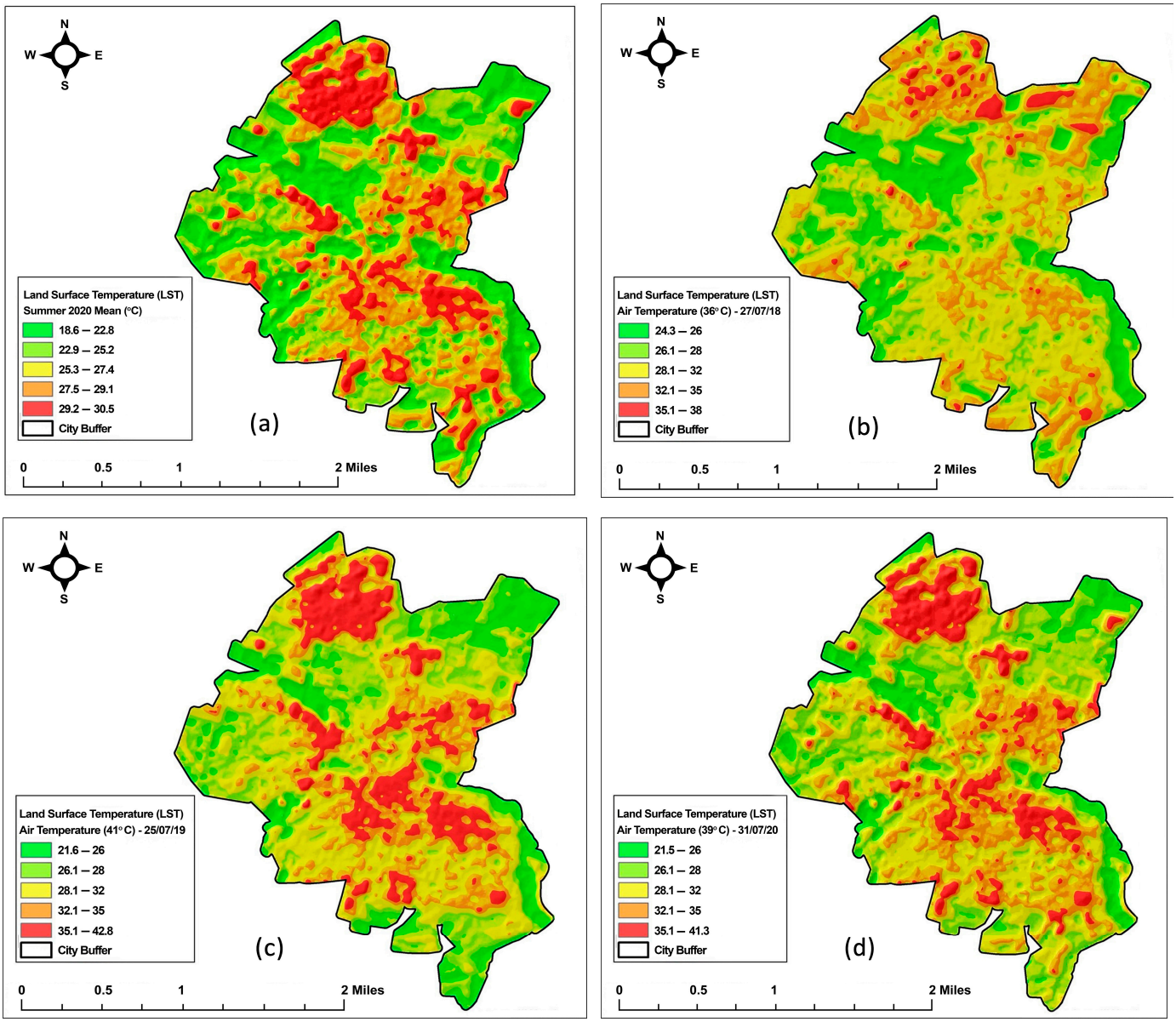

Figure 6. Land surface temperature maps: (**a**) summer mean 2020; (**b**) 27 July 2018; (**c**) 25 July 2019; (**d**) 31 July 2020. Note: The summer mean temperature is the mean LST of July and August 2020.

Table 2. LULC of Amiens.

S.No.	Class	Area (%)	Category for PCA	Total Area (%)
1	Artificial surfaces	31.65	Built-up area	31.65
2	Coniferous tree cover	1.17	Vegetation	56.88
3	Cultivated areas	26.69		
4	Deciduous tree cover	9.29		
5	Herbaceous vegetation	3.93		
6	Moors and heathland	15.80		
7	Natural material surfaces	1.99	Open areas	1.99
8	Marshes	4.68	Wetlands	2.22
9	Peatbogs	2.54		
10	Water bodies	2.26	Water	2.26
	Total	100		100

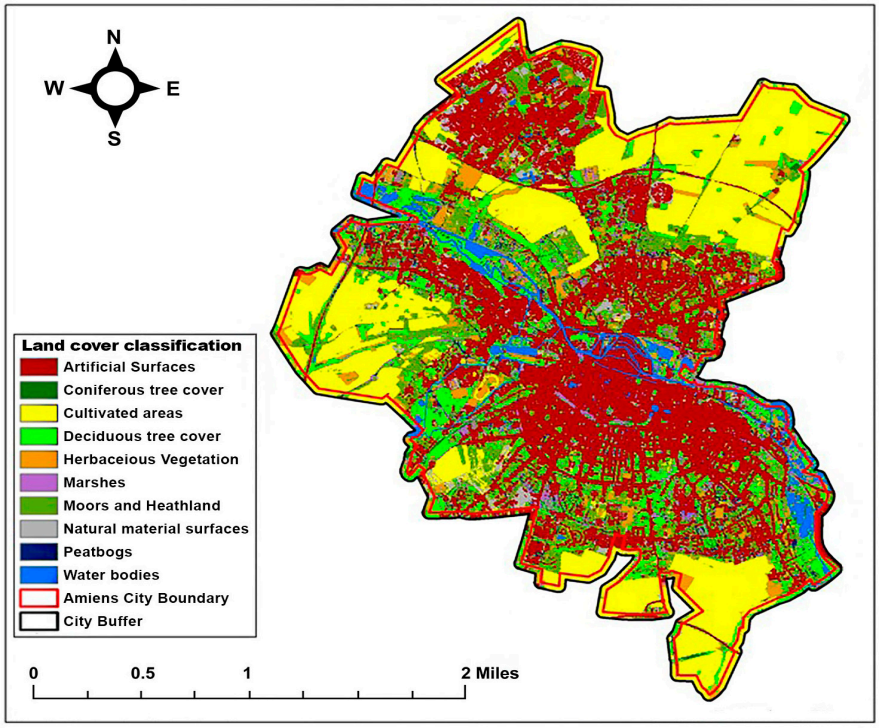

Figure 7. Land use/land cover map of Amiens.

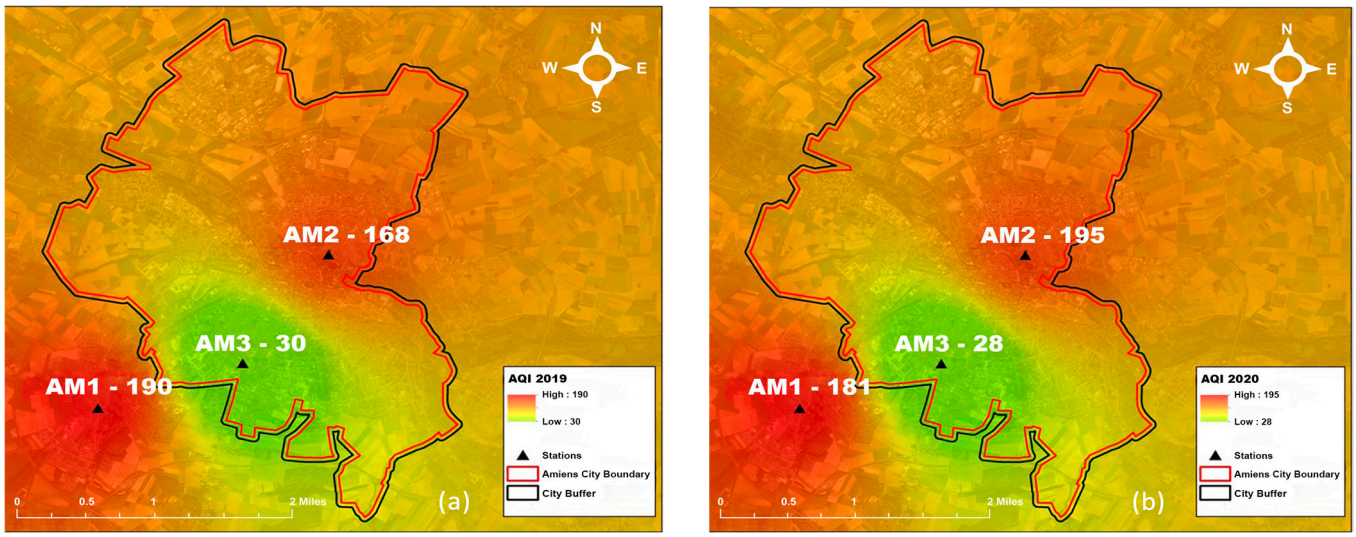

Figure 8. Air quality index maps created with the available data provided by a local agency (Atmo) (**a**) 2019 and (**b**) 2020.

2.2. Principal Component Analysis (PCA)

PCA is typically used in heat vulnerability studies to reduce the number of indicators. We applied this method in Stata v.16, which is an integrated statistical software package used for data analysis, management, and graphing. Stata's PCA was used to estimate the parameters of principal component models, where increasing variables and higher component scores indicated higher HVI. The 32 vulnerability indicators were grouped into five independent components. The variables in the components were allocated via the PCA algorithm [32].

3. Results

3.1. Data Analysis

A linearity between extreme heat events and ground-level ozone concentrations was observed according to the recorded data at AM1 = 157 $\mu g/m^3$, AM2 = 145 $\mu g/m^3$ on 25 July 2019 and at AM1 = 154.9 $\mu g/m^3$, AM2 = 164.5 $\mu g/m^3$ on 31 July 2020 at 3:00 p.m.

After a detailed analysis, we observed that air temperature and ozone data were correlated with significant coefficient (0.8) at the abovementioned stations during the extreme heat days in 2019 and 2020. Due to missing air quality data, heat days in 2018 could not be compared with poor-air-quality events.

3.2. Factor Scores

The factor scores were calculated, and it can be observed that the cumulative contribution of the components was 89.20%, which shows that the proportion of variance of the raw vulnerability indicators captured by PCs were explained by five independent components; for each variable, the sum of its squared loading across all PCs was equal to 1. Mathematically, the loadings were equal to the coordinates of the variables divided by the square root of the eigenvalues associated with the component. The first component explained 44.97% of the total variance, followed by 25.23%, 11.48%, 4.18%, and 3.34% for the second, third, fourth, and fifth components, respectively, as shown in Table 3.

Table 3. The cumulative contribution of variables.

	Extraction Sums of Squared Loadings			
Factors	**Eigenvalue**	**Difference**	**Proportion**	**Cumulative**
1	14.39	6.31	0.45	0.44
2	8.07	4.40	0.25	0.70
3	3.67	2.33	0.11	0.81
4	1.34	0.27	0.04	0.85
5	1.07	0.26	0.03	0.89

The first component included 22 variables (total population, no. of habitants aged ≥65 years, approximate no. of old habitants having asthma, cardiovascular diseases, and other respiratory diseases, no. of socially vulnerable people in the summertime, artificial surfaces in the city, area covered by vegetation, average AQI (N_2, NO, O_3, PM_{10}), illiteracy and poverty rates, and LST of extremely hot days recorded in 2019–2020). The second component was characterized by two variables (mean AQI calculated in the summers of 2019 and 2020). Component 3 was characterized by six variables (NDWI, NDVI, area covered by water bodies, LST of the hottest day in 2018, and summer mean LST of 2020). Components 4 and 5 were represented by the mean elevation and natural surfaces of Amiens, respectively. The merged vegetation was different from the NDVI, as well as the average AQI of each type of air pollutant. After aggregating components into the final HVI through different weight factors, the spatial distribution of HVI was obtained as shown in the map in Figure 9. The distribution of data for each point is provided in Table A2, where factor loadings of variables greater than ±0.6 played an important role in the allocation of variables into defined components via PCA.

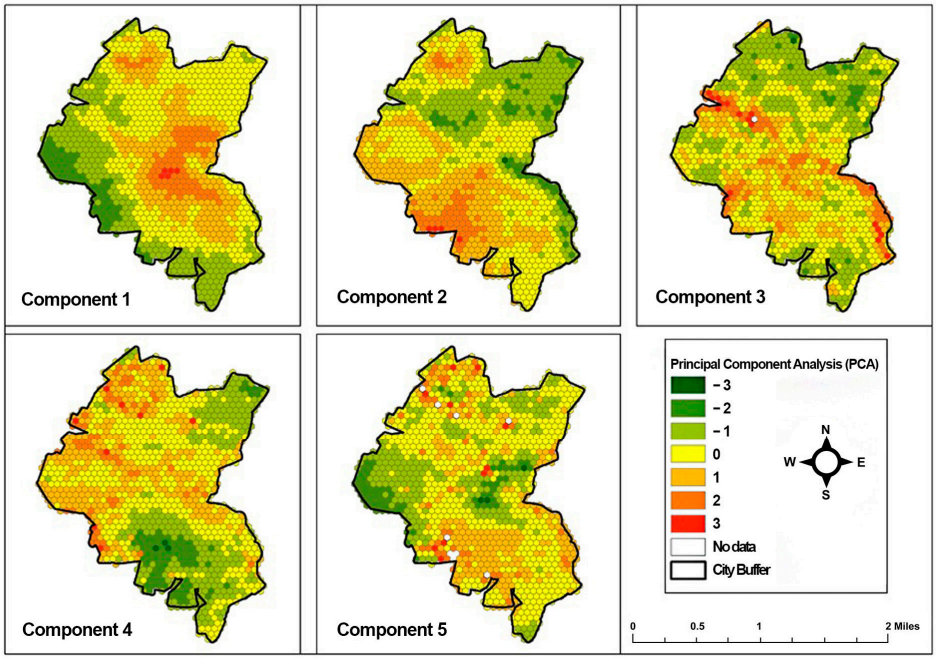

Figure 9. Map of components allocated by PCA algorithm.

3.3. Spatial Derivation Distribution of Heat Vulnerability Index (HVI)

HVI was derived from the sum of all components, and the resultant index map can be seen in Figure 10, where the accumulation of high scores shows that the city center is more vulnerable than rural areas. There may be several possible explanations for our result. The high number of elders and those living alone are concentrated in the city center. Meanwhile, there is a lack of awareness about extreme events and a high poverty rate in suburbs compared to the central area. Moreover, when asphalt is exposed to the sun, pavements start to soften, which can lead to delays and some roads being closed for traffic. This makes the city center more vulnerable to heat stress and poor-air-quality events. The agricultural land also has a high tendency to capture heat due to bare soil and harvesting grains, which causes an increase in HVI during extreme heat days of summer.

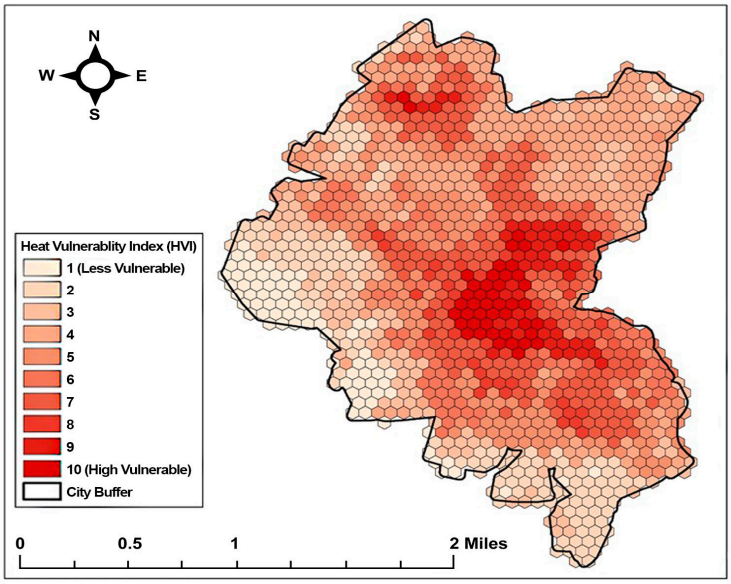

Figure 10. HVI map of Amiens indicating the greater vulnerability of the city center area to heat compared to the rural areas.

4. Discussion

It has been observed that urban vulnerability is linked to various key factors, such as temperature, population, age, gender, literacy and poverty rate, and health-associated problems. It is estimated that, from 1999–2018, the global heat mortality rate increased by 53.7%, resulting in 296,000 deaths in 2018 [33]. By considering the local characters, six important factors were selected to construct the HVI using PCA. These key performance indicators were applied to identify susceptible regions vulnerable to heat waves, as well as population sensitivity and adaptation. This tool can assist in the planning of infrastructure and resources to reduce residents' vulnerability to extreme heat events, especially for the elderly population, since they are more vulnerable and at higher risk of heat-related deaths. The study also highlighted the influence of air pollution on heat events. However, the following limitations and challenges were faced during the development of HVI:

- Irregular and limited monitoring stations of weather and air quality;
- Lack of data from heating and cooling facilities.

The current case study provides a detailed methodology related to the impact of heat stress in the Amiens region, and this approach can be applied to the other regions for understanding the impact of heat waves, serving as a valuable tool for the development of HVI. In this study, our key emphasis was on investigating the adverse effects of strong heat waves on medium-sized cities. In Amiens, a medium-sized French city on which the 2003 heat wave had drastic impacts, it was reported that the annual mean temperature of this city has increased by +1 °C since 2000. A PCA-based novel approach was applied to study the fine-scale vulnerability mapping using various data types, and hotspot zones in the Amiens regions were identified using a comprehensive GIS mapping approach. The analysis identified the elevated HVI in three typical zones, i.e., population-dense and low-vegetation areas, as well as built-up and industrial zones. This was further linked with low vegetation cover, which is greatly responsible for the increasing temperature [34]. Moreover, it is also an established fact that industrialization is a major contributor to global warming [35]. By evaluating multiple covariates influencing the HVI, we are convinced that our current approach may be applicable to other regions of the world, including larger cities, to evaluate the heat-related vulnerabilities and help the authorities to take mitigation measures. Urban greenery and water bodies can be taken as existing cooling strategies; however, for better precision, district cooling consumption data should be considered in future.

5. Conclusions

This work aimed to determine medium-sized city areas with higher heat vulnerability, which are more likely to experience high rates of morbidity and mortality on abnormally warm days. The parameters that influence current heat vulnerability were selected after data analysis and from the scientific literature. A strong relationship was noticed between heat and low air quality. This is a clear illustration of the system theory where anthropogenic activities appear in accordance with the extreme heat events in the city. The PCA technique was very helpful to derive the spatial HVI of the Amiens region. After analyzing the resulting maps, it was observed that the elevated HVI exists particularly in high-density built-up and industrial zones that release thermal energy and ozone at the ground level. A low HVI was located in natural landscapes such as rivers and grasslands. The developed methodology and maps can serve as a powerful tool for an assessment of the effect of extreme heat on vulnerable populations and for communication. It reveals the complex spatial and temporal patterns that would be difficult to interpret through text alone, allowing residents and local stockholders to visualize known areas of high HVI. It can also be influential in decisions to target resources for vulnerable populations to develop adaptation responses that promote resilience.

6. Recommendations

Data fusion techniques are recommended to collect data from multiple sources for analysis and development of HVI, thus increasing reliability and decreasing redundancy to support the decision-making process. This research sheds light on the following solutions that can help citizens to combat heat episodes:

- Information provision to local people about heat warnings and precautions, with more attention to vulnerable people;
- Implementation of proactive adaptive practices such as shades, blue infrastructure, and greenery where the HVI score is above 6;
- Regular monitoring during the summer season in the city.

Author Contributions: The paper was a collaborative effort between the authors. A.M.Q. and A.R. contributed collectively to developing the methodology of this study, analysis, development of HVI and the manuscript preparation. All authors have read and agreed to the published version of the manuscript.

Funding: This paper has been produced within the COOL-TOWNS (Spatial Adaptation for Heat Resilience in Small and Medium Sized Cities in the 2 Seas Region) project which receives funding from the Interreg 2 Seas programme 2014-2020 co-funded by the European Regional Development Fund under subsidy contract N° 2S05-040.

Institutional Review Board Statement: Not applicable

Informed Consent Statement: Not applicable

Conflicts of Interest: The authors declare no conflict of interest.

Appendix A

Table A1. Air quality monitoring and sensor's location.

Name Station	Address of Stations	City	Typology	Remarks
AM1	Rue Anatole France	Salouël	Peri-urban	-
AM2	Parc St Pierre rue Eloi Morel	Amiens	Urban dense	Stopped PM_{25} monitoring in 2018
AM3	Avenue du 14 Juillet	Amiens	Traffic route	Stopped PM_{10} and PM_{25} monitoring in 2018

Table A2. Variable correlation magnitude with each component.

Variable	PC1	PC2	PC3	PC4	PC5	Uniqueness
NDWI	−0.3153	−0.4014	0.6994	−0.0494	0.116	0.2344
NDVI	−0.4412	−0.3843	0.5793	−0.2461	0.0486	0.2591
Total population	0.8145	0.4883	0.2666	−0.0608	−0.1032	0.0128
Age ≥65	0.8145	0.4883	0.2666	−0.0608	−0.1032	0.0128
Age ≥65 + asthma	0.8145	0.4883	0.2666	−0.0608	−0.1032	0.0128
Age ≥65 + respiratory	0.8145	0.4883	0.2666	−0.0608	−0.1032	0.0128
Age ≥65 + cardio	0.8145	0.4883	0.2666	−0.0608	−0.1032	0.0128
Age ≥65 + living alone	0.8145	0.4883	0.2666	−0.0608	−0.1032	0.0128
Artificial surfaces	0.7689	0.4482	0.0143	0.1858	0.0711	0.1682
Natural material	0.0125	0.1735	−0.1649	0.4099	0.6498	0.3523
Water bodies	−0.0301	−0.2768	0.5838	0.2811	0.113	0.4899
Merged vegetation	−0.6601	−0.343	−0.2613	−0.3114	−0.2607	0.2134
Wetlands	0.0924	−0.0937	0.6548	0.0701	0.2628	0.48
Mean_AQI_2019_avg_N_2	0.7961	−0.5903	−0.0698	−0.0861	0.0679	0.0008
Mean_AQI_2019_avg_ NO	0.7961	−0.5903	−0.0698	−0.0861	0.0679	0.0008
Mean_AQI_2019_avg_O_3	−0.7961	0.5903	0.0698	0.0861	−0.0679	0.0008
Mean_AQI_2019_avg_PM_{10}	−0.7961	0.5903	0.0698	0.0861	−0.0679	0.0008
Max_AQI_2019_Max_O_3	−0.7877	0.6026	0.0795	0.0773	−0.0605	0.0006
Mean_AQI_2020_avg_N_2	0.7961	−0.5903	−0.0698	−0.0861	0.0679	0.0008
Mean_AQI_2020_avg_NO	0.7961	−0.5903	−0.0698	−0.0861	0.0679	0.0008
Mean_AQI_2020_avg_O_3	0.7961	−0.5903	−0.0698	−0.0861	0.0679	0.0008
Mean_AQI_2020_avg_PM_{10}	−0.7961	0.5903	0.0698	0.0861	−0.0679	0.0008
Max_AQI_2020_Max_O_3	0.8039	−0.5772	−0.0601	−0.095	0.0762	0.0021
Mean elevation	−0.199	0.257	−0.5217	−0.5109	0.1721	0.3316
Mean_AQI_2019	0.2481	−0.6447	−0.1689	0.5041	−0.3919	0.0865
Mean_AQI_2020	0.3431	−0.6756	−0.1677	0.4493	−0.3438	0.0777
Illiteracy	0.8145	0.4883	0.2666	−0.0608	−0.1032	0.0128
Poverty	0.8145	0.4883	0.2666	−0.0608	−0.1032	0.0128
LST hottest day 2020	0.5975	0.5702	−0.3591	0.1494	0.1406	0.147
LST hottest day 2019	0.6638	0.5418	−0.2211	0.1996	0.1399	0.1575
LST hottest day 2018	0.3725	0.3529	−0.6882	−0.0702	−0.0506	0.2555
LST summer mean 2020	0.509	0.5079	−0.6212	0.0583	0.0474	0.0915

References

1. Thompson, R.; Hornigold, R.; Page, L.; Waite, T. Associations between high ambient temperatures and heat waves with mental health outcomes: A systematic review. *Public Health* **2018**, *161*, 171–191. [CrossRef] [PubMed]
2. Dosio, A.; Mentaschi, L.; Fischer, E.M.; Wyser, K. Extreme heat waves under 1.5 C and 2 C global warming. *Environ. Res. Lett.* **2018**, *13*, 054006. [CrossRef]
3. Fouillet, A.; Rey, G.; Laurent, F.; Pavillon, G.; Bellec, S.; Guihenneuc-Jouyaux, C.; Clavel, J.; Jougla, E.; Hémon, D. Excess mortality related to the August 2003 heat wave in France. *Int. Arch. Occup. Environ. Health* **2006**, *80*, 16–24. [CrossRef] [PubMed]
4. Maloney, S.K.; Forbes, C.F. What effect will a few degrees of climate change have on human heat balance? Implications for human activity. *Int. J. Biometeorol.* **2011**, *55*, 147–160. [CrossRef] [PubMed]
5. Field, C.B.; Barros, V.; Stocker, T.F.; Qin, D.; Dokken, D.J.; Ebi, K.L.; Mastrandrea, M.D.; Mach, K.J.; Plattner, G.-K.; Allen, S.K.; et al. *Managing the Risks of Extreme Events and Disasters to Advance Climate Change Adaptation: Special Report of the Intergovernmental Panel on Climate Change*; Cambridge University Press: Cambridge, UK, 2012.
6. Poumadere, M.; Mays, C.; Mer, S.L.; Blong, R. The 2003 heat wave in France: Dangerous climate change here and now. *Risk Anal. Int. J.* **2005**, *25*, 1483–1494. [CrossRef] [PubMed]
7. Kosatsky, T. The 2003 European heat waves. *Eurosurveillance* **2005**, *10*, 3–4. [CrossRef] [PubMed]
8. Pascal, M.; Wagner, V.; Corso, M.; Laaidi, K.; Ung, A.; Beaudeau, P. Heat and cold related-mortality in 18 French cities. *Environ. Int.* **2018**, *121*, 189–198. [CrossRef] [PubMed]
9. Heat and Health. Available online: https://www.eea.europa.eu/data-and-maps/indicators/heat-and-health/heat-and-health-assessment-published (accessed on 22 April 2022).
10. Weather Amiens, Meteo France. Available online: https://meteofrance.com/previsions-meteo-france/amiens/80000 (accessed on 16 January 2021).
11. Trends in Temperature since 1900 in and around Amiens. Available online: https://do49kvm5ac8w.cloudfront.net/cititexts2019/es/Amiens.html (accessed on 6 December 2021).
12. Karimi, M.; Nazari, R.; Dutova, D.; Khanbilvardi, R.; Ghandehari, M. A conceptual framework for environmental risk and social vulnerability assessment in complex urban settings. *Urban Clim.* **2018**, *26*, 161–173. [CrossRef]
13. City of Philadelphia. Available online: https://www.phila.gov/2019-07-16-heat-vulnerability-index-highlights-city-hot-spots/ (accessed on 16 July 2019).
14. Wolf, T.; McGregor, G. The development of a heat wave vulnerability index for London, United Kingdom. *Weather. Clim. Extrem.* **2013**, *1*, 59–68. [CrossRef]
15. Bodilis, C.; Yenneti, K.; Hawken, S. (2018): Heat Vulnerability Index for Sydney. City Futures Research Centre, UNSW Sydney. Dataset. Available online: https://cityfutures.ada.unsw.edu.au/cityviz/heat-vulnerability-index-sydney/ (accessed on 12 December 2021).
16. Sabrin, S.; Karimi, M.; Nazari, R. Developing Vulnerability Index to Quantify Urban Heat Islands Effects Coupled with Air Pollution: A Case Study of Camden, NJ. *ISPRS Int. J. Geo-Inf.* **2020**, *9*, 349. [CrossRef]
17. Mallen, E.; Stone, B.; Lanza, K. A methodological assessment of extreme heat mortality modeling and heat vulnerability mapping in Dallas, Texas. *Urban Clim.* **2019**, *30*, 100528. [CrossRef]
18. France Population. Available online: https://www.worldpop.org/geodata/summary?id=26330 (accessed on 2 July 2021).
19. Muncipality of Ameins. Available online: https://www.insee.fr/fr/statistiques/2011101?geo=COM-80021 (accessed on 8 December 2021).
20. City Population. Available online: https://www.citypopulation.de/en/france/somme/amiens/80021__amiens/ (accessed on 2 July 2021).
21. Jounieaux, V.; Guillaume, C.; Malka, M.; Wursthorn, M.; Girod, I.; Baron-Papillon, F. Evaluation médico-économique d'un programme de prise en charge de patients asthmatiques. *St. Publique* **2003**, *15*, 449–464. [CrossRef]
22. Tribouilloy, C.; Rusinaru, D.; Mahjoub, H.; Goissen, T.; Lévy, F.; Peltier, M. Impact of echocardiography in patients hospitalized for heart failure: A prospective observational study. *Arch. Cardiovasc. Dis.* **2008**, *101*, 465–473. [CrossRef] [PubMed]
23. Eurostat. Available online: https://ec.europa.eu/eurostat/web/products-eurostat-news/-/edn-20210924-1 (accessed on 21 August 2020).
24. Euro Statistics. Available online: https://ec.europa.eu/eurostat/statistics-explained/index.php?title=File:Share_of_the_population_reporting_that_they_had_chronic_lower_respiratory_diseases_(excluding_asthma),_2014_(%25)_Health20.png (accessed on 21 August 2020).
25. Halima, The City of Amiens Watches over Our Seniors. Available online: https://france3-regions.francetvinfo.fr/hauts-de-france/picardie/somme/amiens/ville-amiens-veille-nos-aines-781919.html (accessed on 8 December 2020).
26. Atmo Hauts de France. Available online: https://www.atmo-hdf.fr/ (accessed on 8 April 2021).
27. ESRI, ARCGIS Software. Available online: https://www.esri.com/en-us/arcgis/products/unlock-earths-secrets (accessed on 8 December 2021).
28. USGS Science for Changing World. Available online: https://earthexplorer.usgs.gov/ (accessed on 21 October 2020).
29. Landsat Collection 2 Surface Temperature. Available online: https://www.usgs.gov/landsat-missions/landsat-collection-2-surface-temperature (accessed on 8 December 2021).

30. Ivajnšič, D.; Kaligarič, M.; Žiberna, I. Geographically weighted regression of the urban heat island of a small city. *Appl. Geogr.* **2014**, *53*, 341–353. [CrossRef]
31. Air Quality Index Calculator. Available online: https://www.airnow.gov/aqi/aqi-calculator-concentration/ (accessed on 10 May 2021).
32. Li, L.; Liu, S.; Peng, Y.; Sun, Z. Overview of principal component analysis algorithm. *Optik* **2016**, *127*, 3935–3944. [CrossRef]
33. Watts, N.; Amann, M.; Arnell, N.; Ayeb-Karlsson, S.; Beagley, J.; Belesova, K.; Boykoff, M.; Byass, P.; Cai, W.; Campbell-Lendrum, D.; et al. The 2020 report of the Lancet Countdown on health and climate change: Responding to converging crises. *Lancet* **2021**, *397*, 129–170. [CrossRef]
34. Van de Walle, J.; Brousse, O.; Arnalsteen, L.; Brimicombe, C.; Byarugaba, D.; Demuzere, M.; Jjemba, E.; Lwasa, S.; Misiani, H.; Nsangi, G.; et al. Lack of vegetation exacerbates exposure to dangerous heat in dense settlements in a tropical African city. *Environ. Res. Lett.* **2022**, *17*, 024004. [CrossRef]
35. Bhattacharjee, P.K. Global warming impact on the earth. *Int. J. Environ. Sci. Dev.* **2010**, *1*, 219. [CrossRef]